Graphite Materials Prepared from an Anthracite: A Structural Characterization

ARTICLE *in* ENERGY & FUELS · JULY 2003

Impact Factor: 2.79 · DOI: 10.1021/ef0300491

3 AUTHORS, INCLUDING:

A.B. Garcia
Spanish National Research Council
68 PUBLICATIONS **834** CITATIONS

SEE PROFILE

Graphite Materials Prepared from an Anthracite: A Structural Characterization

David González, Miguel A. Montes-Morán, and Ana B. Garcia*

Instituto Nacional del Carbón, CSIC, Francisco Pintado Fe 26, 33011 Oviedo, Spain

Received February 25, 2003. Revised Manuscript Received July 8, 2003

The purpose of this research was to study the influence of the temperature, treatment time, and initial coal particle size on the evolution of the structural order of graphite materials that have been prepared from an anthracite at temperatures >2273 K. Crystalline parameters such as the interlayer spacing and crystallite sizes were calculated from X-ray diffractometry measurements. The analysis of the first- and second-order Raman spectra allowed the assessment of the degree of orientation at the outermost layers of these materials. The graphitization of the anthracite happened in two different stages. The temperature of 2673 K seems to be the inflection point for the change in the graphitization rate of the anthracite. Highly crystalline materials were obtained at 2673 K. Temperatures of treatment >2673 K led to minor changes in the degree of structural order of the graphite materials obtained. The initial particle size of the anthracite affected the evolution of the graphitization process with temperature, because of differences in the ratio of particles that contain organic matter and mineral matter associations. The degree of graphitization achieved with this coal was comparable to that of other natural and synthetic graphites.

Introduction

Synthetic graphite has a wide range of applications, from the manufacture of electrodes for aluminum and steel industries (which amounts to a significant portion of the market) to high-technology uses such as applications in fuel cells and lithium ion batteries.[1,2] The use of synthetic graphite is increasing worldwide. Thus, the global demand for graphite, including both natural and synthetic, to be used in mobile energy storage systems is expected to grow more than 100 000 tons per year.[2−4] The graphite production process involves the selection of carbon materials (precursors) that graphitize readily. Currently, petroleum coke of various grades is used as the main filler material in the manufacturing of synthetic graphite.[5]

Coal is an important source of energy and an abundant source of carbon; known world reserves for consumption are >215 years, versus a time of 39 years for petroleum.[6] Therefore, an increasing number of high valuable carbon materials are being produced from coal. Among the different classes of coals, anthracites seem to be potential precursor materials for graphite. Typical carbon contents of anthracites are well over 90%, which is arranged in a macromolecular structure of condensed aromatic rings that form large units (graphene layers) bridged or "cross-linked" by aliphatic and/or ether groups,[7] conferring them a certain structural order. The removal of the "cross links" by heating the anthracite at high temperature should facilitate the reorganization of the aromatic units into graphitelike structures. Previous studies have demonstrated that anthracites can graphitize when heated at temperatures >2273 K.[8,9] Thus, graphite materials with an acceptable degree of structural order were obtained from anthracites of different origin at temperatures ≥2973 K.[10−14]

In addition to the temperature of treatment, some characteristics of the anthracite influence the graphitization process. Thus, the coal mineral matter has been suggested to act as a graphitization catalyst,[8,9] whereas more-ordered materials were prepared from anthracites with a higher H/C atomic ratio, inferring the influence of the elemental composition on their graphitization.[14]

* Author to whom correspondence should be addressed. E-mail: anabgs@incar.csic.es.

(1) Pierson, H. O. *Handbook of Carbon, Graphite, Diamond and Fullerene*; Noyes: Park Ridge, NJ, 1993; pp 87−121.
(2) Kalyoncu, R. S. *Graphite*; U. S. Geological Survey Minerals Yearbook; U.S. Department of Interior: Reston, VA, 2001; pp 341−343.
(3) Pan, Q.; Guo, K.; Wang, L.; Fang, S. *J. Mater. Chem.* **2002**, *12*, 1833−1838.
(4) Wu, Y.; Jiang, C.; Wan, C.; Tsuchida, E. *J. Mater. Chem.* **2001**, *11*, 1233−1236.
(5) Mantel, C. L. *Carbon and Graphite Handbook*; Interscience Publishers: New York, 1968; pp 319−330.
(6) Schobert, H. H.; Song, C. *Fuel* **2002**, *81*, 15−32.
(7) van Krevelen, D. W. *Coal: Typology, Physics, Chemistry and Constitution*; Elsevier: Amsterdam, 1993; pp 777−810.
(8) Oberlin, A.; Terriere, G. *Carbon* **1975**, *13*, 367−376.
(9) Evans, E. L.; Jenkins, J. L.; Thomas, J. M. *Carbon* **1972**, *10*, 637−642.
(10) Ruber, S.; Rouzaud, J. N.; Beny, C.; Dumas, D. *21st Biennial Conference on Carbon: Extended Abstracts*; American Carbon Society: Buffalo, NY, 1993; p 317.
(11) Zeng, S. M.; Rusinko, F.; Schobert, H. H. *Carbon '95: 22nd Biennial Conference on Carbon: Extended Abstracts*; American Carbon Society: San Diego, CA, 1995; p 692.
(12) Atria, J.; Zeng, S. M.; Schobert, H. H.; Rusinko, F. D. *21st Biennial Conference on Carbon: Extended Abstracts*; American Carbon Society: Buffalo, NY, 1993; p 342.
(13) Bustin, R. M.; Ross, J. V.; Rouzaud, J. N. *Int. J. Coal Geol.* **1995**, *28*, 1.
(14) Atria, J. V.; Rusinko, F., Jr.; Schobert, H. H. *Energy Fuels* **2002**, *16*, 1343.

10.1021/ef0300491 CCC: $25.00
Published on Web 07/30/2003

The microtexture of the anthracite was also related to its ability to graphitize, specifically when there is a preferential planar orientation of the polyaromatic basic structural units.[15] Graphite formation has been suggested to occur as a consequence of the improvement of pore flattening during heating.[8,16]

In the work described in this paper, an anthracite at two different particle sizes was heated at temperatures of 2273, 2473, 2673, 2773, 2883, 2973, and 3073 K, for the purpose of exploring its ability to graphitize. This is the critical temperature range in which the graphitization of anthracites occurs. The influence of the treatment temperature and time, and initial coal particle size, on the evolution of the crystallinity and orientation of the graphite materials obtained was evaluated by X-ray diffraction (XRD) and Raman spectroscopy, respectively. Helium densities were also used to estimate the structural characteristics of the graphitization products, given that the presence in the graphite materials of imperfections leads to lower densities.[17]

Typical crystalline parameters, such as interlayer spacing (d_{002}) and crystallite sizes along the *c*-axis (L_c) and in the layer sheet direction (L_a) calculated from XRD, are used to assess the crystallinity of graphite materials obtained from different precursors.[18−22] Raman spectroscopy has been used extensively as a surface characterization technique for carbon material.[20,23−27] This analysis method combines a prominent surface selectivity (the depth of analysis and spatial resolution have been estimated to be a few hundred angstroms and 1−2 μm, respectively) with an exceptional sensitivity to the degree of structural order. In addition to the G band that is typical for graphite crystal, carbon materials generally present a second band (D band) in their first-order Raman spectrum, as a consequence of the relaxation of the selection rules, because of the existence of structural disorder. Thus, different parameters such as G bandwidths and D−G band intensity ratios are used to quantify the degree of disorder in this type of material.[20,23−27] In addition, analysis of the second-order region of the Raman spectra seems to provide useful information related to the degree of surface structural order in highly oriented carbon materials.[28] These two techniques have been found to be complementary for the characterization of carbon materials. Indeed, XRD measurements come from a volume of randomly disposed particles, whereas Raman measurements result from a limited volume of a particle surface. The relationships between the different structural parameters obtained from XRD and Raman have been investigated by different authors.[20,25,29]

Experimental Section

Materials. An anthracite, denoted as AF, run-of-mine from Villablino in northwest Spain was selected for this research. Ash and volatile matter (VM) contents (weight percent, dry basis) of 19.74 and 8.72, respectively, were determined for the anthracite, with its random reflectance (R_o) being 2.37%. The elemental analysis (weight percent, dry-ash-free basis) is 91.00 carbon, 3.01 hydrogen, 1.40 nitrogen, 0.92 organic sulfur, and 3.87 oxygen (by difference). Representative samples of AF anthracite were ground to top sizes of 212 and 45 μm, prior to the graphitization experiments.

Two synthetic graphites (R1, R2) and one natural commercial graphite (R3) were also selected, for comparative purposes. R1 is a graphite powder that was supplied by Fluka (Sigma−Aldrich, Inc.), with a purity >99.9 wt % carbon. R2 and R3 are the EP1200 and EDM96/97 powder graphites provided by Richard Anton KG (München, Germany), with purities of >99.2 and >95.0 wt %, respectively.

Graphitization. The AF anthracite was carbonized at 1273 K in a tube furnace, under a nitrogen flow, for 1 h with a heating rate of 2 K/min, and then was graphitized. The graphitization experiments were conducted at 2273, 2473, 2673, 2773, 2883, 2973, and 3073 K in a graphite furnace for 1−4 h under an argon flow. The heating rates were 20 K/min from room temperature to 2273 K and 10 K/min from 2273 K to the prescribed temperature.

X-ray Diffraction. The diffractograms of the samples were recorded in a Siemens model D5000 powder diffractometer that was equipped with monochromatic Cu Kα X-ray source and had an internal standard of silicon powder. Diffraction data were collected by step scanning with a step size of 0.02° 2θ and a scan step time of 1 s. For each sample, five diffractograms were obtained, using a different representative batch of sample for each run. The interlayer spacing, d_{002}, was evaluated from the position of the (002) peak applying Bragg's equation. The crystallite sizes along the *c*-axis (L_c) and along the *a*-axis (L_a) (basal planes) were calculated from the (002) and (110) peaks, respectively, using the Scherrer formula, with values of $K = 0.9$ for L_c and 1.84 for L_a.[30] The broadening of diffraction peaks due to instrumental factors was corrected with the use of a silicon standard.

Raman Spectroscopy. Raman spectra were obtained in a Raman microspectrometer (Renishaw System 1000) that used the green line of an argon laser ($\lambda = 514.5$ nm) as the excitation source and was equipped with a charge-coupled device (CCD) camera. The 50× objective lens of an Olympus BH-2 optical microscope was used both to focus the laser beam (at a power of ∼25 mW) and to collect the scattered radiation. Extended scans, over a range of 3000−1000 cm^{-1}, were performed to obtain the first- and second-order Raman bands of the samples, with typical exposure times of 30 s. To assess differences within samples, at least 21 measurements were performed on different particles of each individual sample. The intensity *I*, width *W*, and frequency ν of the bands were measured using a mixed Gaussian−Lorentzian curve-fitting procedure.

Helium Density. Density measurements of the samples were made with a helium pycnometer (Micromeritics model Accupyc 1330).

(15) Blanche, C.; Rouzaud, J. N.; Dumas, D. *Carbon '95: 22nd Biennial Conference on Carbon: Extended Abstracts*; American Carbon Society: San Diego, CA, 1995; p 694.
(16) Deurbergue, A.; Oberlin, A.; Oh, J. H.; Rouzaud, J. N. *Int. J. Coal Geol.* **1987**, *8*, 375.
(17) Pierson, H. O. *Handbook of Carbon, Graphite, Diamond and Fullerene*; Noyes: Park Ridge, NJ, 1993; pp 43−69.
(18) Kajiura, K.; Tanabe, Y.; Yasuda, E. *Carbon* **1997**, *35*, 1169.
(19) Oberlin, A. *Carbon* **1984**, *22*, 521.
(20) Cuesta, A.; Dhamelincourt, P.; Laureyns, J.; Martínez-Alonso, A.; Tascón, J. M. D. *J. Mater. Chem.* **1998**, *8*, 2875.
(21) Franklin, R. E. *Acta Crystallogr.* **1951**, *4*, 253.
(22) Bourrat, X. In *Sciences of Carbon Materials*; Marsh, H., Rodriguez-Reinoso, F., Eds.; University of Alicante: Alicante, Spain, 2000; pp 1−97.
(23) Waldek Zerda, T.; Gruber, T. *Rubber Chem. Technol.* **2000**, *73*, 284.
(24) Tunistra, F.; Koening, J. L. *J. Chem. Phys.* **1970**, *53*, 1126.
(25) Lespade, P.; Marchand, A.; Couzi, M.; Cruege, F. *Carbon* **1984**, *22*, 375.
(26) Cuesta, A.; Dhamelincourt, P.; Laureyns, J.; Martínez-Alonso, A.; Tascón, J. M. D. *Carbon* **1994**, *32*, 1523.
(27) Montes-Morán, M. A.; Young, R. J. *Carbon* **2002**, *40*, 845.
(28) Angoni, K. *J. Mater. Sci.* **1998**, *33*, 3693.
(29) Gruber, T.; Waldek Zerda, T.; Gerspacher, M. *Carbon* **1994**, *32*, 1377.
(30) Biscoe, J.; Warren, B. *J. Appl. Phys.* **1942**, *13*, 364.

Table 1. XRD Crystallographic Parameters and Helium Density Values of the Graphite Materials Prepared from AF Anthracite and Reference Graphites

	temp (K)/ time (h)	d_{002} (nm)	L_c (nm)	L_a (nm)	helium density (g/cm^3)
		Anthracite			
AF ≤212 μm	2273/1	0.3395	8.3	29.7	1.89
AF ≤212 μm	2473/1	0.3391	8.9	35.2	1.92
AF ≤212 μm	2673/1	0.3368	18.5	49.1	2.04
AF ≤212 μm	2773/1	0.3373	17.6	51.0	2.04
AF ≤212 μm	2873/1	0.3373	17.3	48.4	2.04
AF ≤212 μm	2973/1	0.3371	17.2	50.5	2.06
AF ≤212 μm	3073/1	0.3372	18.2	48.2	2.07
AF ≤45 μm	2273/1	0.3397	7.3	29.2	1.84
AF ≤45 μm	2473/1	0.3384	9.8	46.3	1.96
AF ≤45 μm	2673/1	0.3378	16.6	46.3	2.02
AF ≤45 μm	2773/1	0.3374	18.1	47.2	2.06
AF ≤45 μm	2873/1	0.3374	18.4	48.0	2.10
AF ≤45 μm	2973/1	0.3366	20.0	48.2	2.10
AF ≤45 μm	2973/2	0.3369	20.3	54.4	2.11
AF ≤45 μm	2973/3	0.3365	19.7	46.3	2.11
AF ≤45 μm	2973/4	0.3367	18.7	48.2	2.10
		Graphites			
R1		0.3358	25.8	47.4	2.32
R2		0.3361	28.3	58.0	2.29
R3		0.3364	24.3	47.3	2.32

Table 2. Positions (ν_i) and Widths (fwhm) (W_i) of the First-Order Raman Bands Measured for the Graphite Materials Prepared from AF Anthracite and Reference Graphites[a]

	temp (K)/ time (h)	D Band		G Band		D′ Band	
		ν_D	W_D	ν_G	W_G	$\nu_{D'}$	$W_{D'}$
		Anthracite					
AF ≤212 μm	2273/1	1352.5	45.9	1582.1	32.0	1618.9	27.3
AF ≤212 μm	2473/1	1353.5	41.9	1581.1	26.5	1618.6	22.8
AF ≤212 μm	2673/1	1353.9	43.6	1579.6	21.0	1615.1	21.7
AF ≤212 μm	2773/1	1354.4	40.9	1580.3	21.0	1618.8	18.8
AF ≤212 μm	2873/1	1353.4	38.8	1579.4	21.3	1616.8	17.0
AF ≤212 μm	2973/1	1354.9	44.5	1580.8	20.5	1616.3	23.5
AF ≤212 μm	3073/1	1355.6	36.1	1580.4	20.7	1613.7	18.9
AF ≤45 μm	2273/1	1352.6	48.2	1581.6	36.1	1618.2	27.4
AF ≤45 μm	2473/1	1353.5	45.1	1581.4	28.6	1618.9	23.9
AF ≤45 μm	2673/1	1354.2	47.9	1579.9	21.2	1615.6	25.3
AF ≤45 μm	2773/1	1354.6	46.1	1580.2	21.8	1614.8	26.9
AF ≤45 μm	2873/1	1353.4	44.3	1579.1	22.2	1614.6	24.0
AF ≤45 μm	2973/1	1354.0	45.9	1579.4	20.3	1614.7	25.0
AF ≤45 μm	2973/2	1354.9	41.1	1581.7	20.2	1616.5	19.0
AF ≤45 μm	2973/3	1353.5	34.9	1579.3	21.1	1615.0	18.2
AF ≤45 μm	2973/4	1353.9	40.1	1578.8	19.9	1616.0	17.1
		Graphites					
R1		1351.4	46.1	1578.3	18.6	1608.3	25.1
R2		1352.0	52.1	1580.6	19.5	1608.3	31.7
R3		1352.1	48.6	1579.5	16.8	1608.4	25.8

[a] All ν_i and W_i values are given in units of cm^{-1}.

Results and Discussion

The analysis of the XRD profiles of these graphitized samples showed that, as the temperature increases, the width of the (002) peak gradually decreases and its maximum shifts to larger angles, becoming virtually symmetric with a much higher intensity, the (10) band splits into (100) and (101) well-defined peaks, and an additional (112) diffraction peak appears. These facts are associated with the development of a three-dimensional crystalline structure of graphitic carbon.[21,31] The interlayer spacing d_{002} and crystallite sizes L_c and L_a, as well as the helium densities, of the graphite materials obtained from AF anthracite at particle sizes of ≤212 and ≤45 μm are reported in Table 1. Data corresponding to the reference graphites R1−R3 are also collected in Table 1. Experimental errors are not included in the table for clarity. Typical standard errors of crystallite size measurements are approximately ±8% of the reported values. The d_{002} measurements are much more precise, with standard errors of <0.03%.

The Raman spectra of the graphitized samples from AF anthracite are characteristic of highly oriented carbon materials.[20,23−28] Three well-resolved bands appear in the first-order region (1000−2000 cm^{-1}): a prominent G band (after graphite) at ∼1580 cm^{-1}, a less-intense D band (after defects) at ∼1350 cm^{-1}, and the D′ band close to the main graphitic band (∼1615 cm^{-1}). The second-order region of the Raman spectra (2000−3000 cm^{-1}) presents a composite G′ band that occurs at ∼2700 cm^{-1}, which, in the case of highly graphitized particles, has a tendency to split into a doublet: G'_1 at ∼2695 cm^{-1} and G'_2 at ∼2735 cm^{-1}. Values of the averaged band positions and bandwidths (full width at half-maximum, fwhm) measured for the materials under study are collected in Tables 2 and 3. Similar to that which was shown for the XRD analysis (see Table 1), the Raman parameters of the three graphites of reference are also included in Tables 2 and 3. The band positions are measured with a relatively high precision, with standard errors being ∼0.05%−0.1% of the reported values. Standard errors of the bandwidths are within 2%−4% of the reported values.

Graphitization of AF Anthracite at a Particle Size of ≤212 μm. Two temperature zones may be distinguished in the evolution of the crystallinity of the graphite materials obtained from AF coal at a particle size of ≤212 μm: (i) 2273−2673 K and (ii) >2673 K. Thus, as the graphitization temperature increases from 2273 to 2673 K, the interlayer spacing d_{002} decreases rapidly, attaining a plateau value (∼0.337 nm; see Table 1). Similarly, the crystallite size L_a increases from 30 nm to 50 nm, whereas L_c doubles from 8 nm to 18 nm. Graphitization temperatures of >2673 K do not improve the degree of crystallinity of these materials significantly.

The parameters obtained from Raman measurements also confirm this two-stage graphitization process. In the first-order spectrum region (see Table 2), the fwhm of the G band (W_G) decreases from 32 cm^{-1} at 2273 K to 21 cm^{-1} at 2673 K and does not change significantly at higher treatment temperatures. Because a surface formed by highly orientated crystallites would result from a narrower phonon distribution, the narrowing of the G band could be related to an increase of the size and/or orientation of the graphitic domains. Moreover, the decay of the relative intensity of the D band also indicates an improvement of the crystallite orientation of the graphite materials.[20,23−28] Figure 1 shows the two-step variation of I_D/I_t ($I_t = I_D + I_G + I_{D'}$) graphically, with the plateau value being 13%−14%.

Bands in the second-order region of the Raman spectrum are only observable in highly oriented carbon materials. Therefore, some parameters have been proposed to account for the degree of crystallite orientation in the surface of graphitelike materials.[28] The G′ band has been observed initially to narrow as the surface order of the material increases. At a given level of

(31) Pierson, H. O. *Handbook of Carbon, Graphite, Diamond and Fullerene*; Noyes: Park Ridge, NJ, 1993; pp 70−86.

Table 3. Positions (ν_i) and Widths (fwhm) (W_i) of the Second-Order Raman Bands Measured for the Graphite Materials Prepared from AF Anthracite and Reference Graphites[a]

		G′ Band		G'_1 Band		G'_2 Band			
	temp (K)/time (h)	$\nu_{G'}$	$W_{G'}$	$\nu_{G'_1}$	$W_{G'_1}$	$\nu_{G'_2}$	$W_{G'_2}$	$\Delta\nu_{G'}$[b]	N[c](%)
				Anthracite					
AF ≤212 μm	2273/1	2703.8	62.2						0
AF ≤212 μm	2473/1	2704.4	51.4						0
AF ≤212 μm	2673/1	2704.9	56.4	2721.1	49.4	2699.2	59.7	21.9	24
AF ≤212 μm	2773/1	2705.6	54.4	2725.8	44.4	2700.2	56.3	25.6	24
AF ≤212 μm	2873/1	2704.4	54.9	2723.9	44.0	2696.2	62.3	27.8	29
AF ≤212 μm	2973/1	2707.6	55.9	2727.2	39.0	2702.6	63.6	24.6	24
AF ≤212 μm	3073/1	2706.2	57.5	2724.7	43.9	2694.1	60.4	30.6	38
AF ≤45 μm	2273/1	2699.8	68.9						0
AF ≤45 μm	2473/1	2703.3	57.7						0
AF ≤45 μm	2673/1	2704.8	58.8	2718.3	49.3	2697.1	57.8	19.2	9.5
AF ≤45 μm	2773/1	2704.6	54.9	2731.8	28.4	2703.9	74.8	25.9	5
AF ≤45 μm	2873/1	2703.5	59.2	2722.8	44.3	2698.9	59.8	21.9	9.5
AF ≤45 μm	2973/**1**	2702.1	56.3	2723.7	42.2	2697.2	65.0	24.4	33
AF ≤45 μm	2973/**2**	2708.7	56.7	2732.3	32.9	2704.8	68.1	25.5	20
AF ≤45 μm	2973/**3**	2703.5	60.4	2722.5	40.5	2698.0	70.8	22.4	33
AF ≤45 μm	2973/**4**	2703.2	64.5	2725.4	39.9	2701.6	68.6	21.7	28.5
				Graphites					
R1				2725.2	41.7	2693.4	65.2	31.8	100
R2				2729.3	39.8	2698.0	72.1	29.3	100
R3				2726.9	38.4	2686.1	55.5	38.8	100

[a] All ν_i and W_i values are given in units of cm^{-1}. [b] $\Delta\nu_{G'} = \nu_{G'_1} - \nu_{G'_2}$. [c] Percentage of particles exhibiting the G'_1, G'_2 doublet (see text).

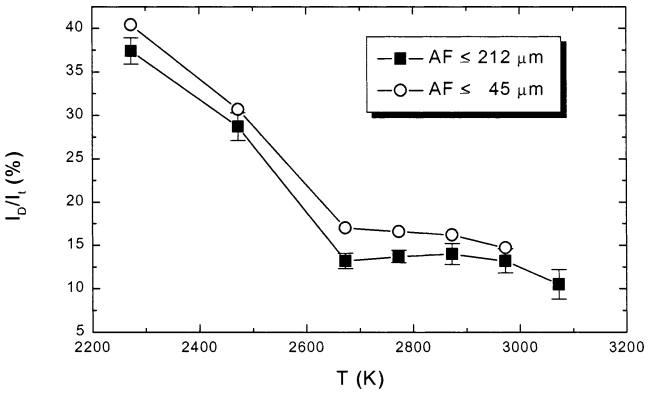

Figure 1. Values of the relative intensity of the Raman D band (I_D/I_t) calculated for the graphite materials prepared from AF anthracite.

crystal orientation, the same band starts to widen until it splits into a doublet for graphite materials with none or few defects along their graphene layers (see $W_{G'}$ in Table 3). Because of the heterogeneity of the samples studied, the number percentage of particles (or measurement areas) that exhibit the G′ band doublet should constitute an indication of the degree of crystallite order for a given material. That percentage is shown in the last column of Table 3 for the graphitized samples of AF anthracite. Again, the values obtained support the idea of a two-step graphitization process: no particles with G'_1, G'_2 doublets were detected until the AF ≤212 μm coal was heated at 2673 K, then attaining a plateau value of 25%−30% within the temperature range of 2673−2973 K.

Significantly, however, the sample graphitized at the highest temperature (3073 K) displays an increase (up to 38%) in the number of particles showing a doublet of the 2700 cm^{-1} second-order Raman band (see Table 3). This would also agree with the I_D/I_t values (see Figure 1), where a noticeable decrease is observed for the sample that was treated at 3073 K. Using an empirical basis, Angoni proposed that the differences between the positions of the G'_1 and G'_2 bands can be used as a sensitive feature to identify changes after structural modifications of highly ordered carbon materials: the higher the shift, the higher the level of structural orientation.[28] This shift ($\Delta\nu_{G'}$) has been calculated for the Raman spectra of the materials under consideration, the averages of which are collected in Table 3. These results seem to confirm that, regardless of the crystallographic measurements (see Table 1), the treatment at 3073 K slightly improves the level of structural order of the graphite material obtained.

The two-step graphitization process has also been reported to happen during an extensive characterization of the graphite materials that are obtained from a very different precursor: polyimide films.[32−34] The two precursors (anthracites and polyimides) undergo a solid-state type of carbonization in the early stages of the graphitization process. The "flattening-pore" model, which is based on transmission electron microscopy (TEM) observations,[8,16,32] has been proposed to account for the two different rates of graphitization that have been discussed already. According to this model, basic structural units (or nanocrystallites) arrange around the walls of pores that would flatten progressively as the temperature increases. A preferential lateral coalescence of the crystallites occurs in this stage, as confirmed by an absolute growth of the crystal size L_a being greater than that of L_c (see Table 1). The walls of the pores would collapse at a given temperature, leading to a sudden increase of the three-dimensional order. In the present study, this seems to happen at a temperature within the range of 2473−2673 K. Thus, L_c *proportional* growth (from ∼9 nm to 18 nm; see Table 1) is higher than that observed in the basal plane

(32) Inagaki, M.; Takeichi, T.; Hishiyama, Y.; Oberlin, A. In *Chemistry and Physics of Carbons*; Thrower, P. A., Radovic, L. R., Eds.; Marcel Dekker: New York, 1999; pp 245−333.
(33) Bourgerette, C.; Oberlin, A.; Inagaki, M. *J. Mater. Res.* **1992**, *7*, 1158.
(34) Bourgerette, C.; Oberlin, A.; Inagaki, M. *J. Mater. Res.* **1993**, *8*, 121.

a-direction. After the pores have collapsed, further improvement of the degree of crystallinity is very slow (see Table 1, Figure 1). A temperature of 2573 K has been quoted as the limiting temperature at which the transition from turbostratic to graphitic structures occurs in the case of the polyimide films graphitization,[32] which compares well to our findings in the graphitization of AF anthracite.

Graphitization of AF Anthracite at a Particle Size of ≤45 μm. A comparative analysis of the graphitization results leads one to conclude that materials with a similar degree of crystallinity and structural orientation can be obtained from AF coal at both particle sizes (see Tables 1−3). The aforementioned two-step graphitization process is also noticeable in the present case, as clearly shown in Figure 1. However, close inspection of the XRD structural data and Raman parameters reveals a difference between the graphite materials obtained from AF anthracite at ≤212 and ≤45 μm. This difference concerns the evolution of the graphitization process at temperatures >2673 K. Regarding the average crystal parameters, a slight decrease of the d_{002} value of the materials from AF anthracite at the lowest particle size of ≤45 μm occurs. For example, d_{002} values of 0.3378 and 0.3366 nm are obtained for samples of AF ≤45 μm coal that have been heated to 2673 and 2973 K, respectively. A small increase of the crystallite sizes L_a and L_c can be also observed within this temperature range. On the other hand, the d_{002}, L_c, and L_a values of the graphitized samples from AF ≤212 μm coal remain almost unchanged in the temperature range of 2673−3073 K.

The results from the Raman experiments partially confirm the previous observations. Thus, for the graphite materials that are produced from the AF ≤45 μm anthracite, the number of particles that present the doublet in the second-order region, the doublet shift $\Delta\nu_{G'}$ (see Table 3), and the variations of I_D/I_t values (see Figure 1) follow trends that indicate an improvement of the structural order as the treatment temperature increases, from 2673 K to 2973 K. Only W_G remains unaltered within the temperature range of 2673−2973 K (see Table 2).

This slight difference in the behavior of both series of graphite materials during the second stage of the graphitization process results in an important outcome, from a practical point of view: a higher temperature must be used for the graphitization of AF ≤45 μm anthracite to obtain materials with structural characteristics that are similar to those prepared from the AF ≤212 μm anthracite. This effect of the initial coal particle size can be explained through the heterogeneity of the AF anthracite particles, which confers them a different ability to graphitize. In terms of organic matter/mineral matter composition, two main types of graphitizable particles can be distinguished in coals: free organic matter (OM) particles and particles with associations of organic and mineral matters in different proportions (OM−MM); the latter has an important role in the graphitization process, because of the catalytic effect of some of the constituents of the mineral matter.[8,9,35] In addition to different particle sizes, the two starting samples of AF anthracite also have different proportions of OM−MM particles, as measured by optical microscopy on the polished surface of petrographic pellets by examining at least 1000 particles. Thus, as a consequence of the higher grindability of the organic matter of the coals, the number percentage of OM−MM particles decreases from 23% in AF ≤212 μm to only 5% in AF ≤45 μm. The presence in AF ≤212 μm coal of a much greater amount of OM−MM particles, in which there exists an intrinsic association between the two matters of coal, may improve the catalytic effect of the mineral matter. This would lead to materials with better (more graphitelike) structural properties at a lower temperature. In this sense, graphitized regions that surround mineral particles were previously found in heat-treated anthracites at temperatures as low as 1573 K.[9]

A final remark from the study of the graphitization of AF ≤45 μm anthracite concerns the influence of treatment time on the structural properties of the graphite materials that are obtained. Rather than performing an extensive study, the present work shows the effect of increasing the treatment time of highly graphitized samples, i.e., samples treated at high temperatures (2973 K). Crystallite parameters (see Table 1) are only slightly sensitive to graphitization times >1 h. Thus, d_{002} values of 0.3366 and 0.3367 nm are measured for samples of AF ≤45 μm anthracite that has been graphitized at 2973 K for 1 and 4 h, respectively. The pertinent Raman parameters, which have already mentioned to account for the degree of structural order, also confirm that there is no significant improvement after 1 h of treatment (I_D/I_t values of the AF ≤45 μm anthracite treated at 2973 K for 1, 2, 3, and 4 h are 14.7%, 11.2%, 12.4%, and 13.7%, respectively). It can be concluded from these results that 1 h of heat treatment at 2973 K allows the material to develop its maximum degree of structural order. Thus, the evolution of the crystallinity of these graphite materials is mainly affected by the temperature and it slows after a specific degree of crystallinity has been attained. The temperature of 2673 K seems to be the inflection point for the change in the graphitization rate of AF anthracite.

Comparison to Other Graphites. To complete the present study, it was found interesting to compare the structural characteristics of the graphite materials that were prepared from AF anthracite, already discussed, to those measured for other natural and synthetic graphites. Three graphites, R1−R3, were selected as stated in the Experimental Section, and they were characterized following identical routines to those described therein. XRD results are collected in Table 2, and the Raman parameters appear in Tables 2 and 3.

According to the crystalline parameters obtained, the heat treatment of the AF anthracite at temperatures ≥2673 K results in graphite materials that have properties comparable to those of some natural and synthetic graphites that are commercially available. Thus, d_{002}

(35) Zeng, S. M.; Rusinko, F.; Schobert, H. H. *Producing High-Quality Carbon and/or Graphite Materials from Anthracite by Catalytic Graphitization*; Grant Agreement 9303-4019; Commonwealth of Pennsylvania, Pennsylvania Energy Development Authority: Harrisburg, PA, 1996.

spacings within 0.3369−0.3365 nm, which are very close to the values of graphites R2 and R3, were achieved for samples of AF ≤45 μm heated at 2973 K. L_a crystallite sizes of the highly graphitized AF anthracite samples (∼50 nm) are also within the range of the reference graphites. However, L_c results of the graphitized samples from the amthracite (∼20 nm) are significantly lower than those of the R1−R3 graphites, which indicates a less-developed three-dimensional order.

Comparison of the Raman results highlighted some additional differences between the graphite materials that were prepared and the graphites that were used for reference. The W_G values of graphites R1−R3 are less than those of the graphitized samples (see Table 2). Conversely, the number of particles that exhibit a doublet in the second-order region, and its shift $\Delta\nu_{G'}$, are higher for graphites R1−R3 (see Table 3). Both trends indicate a better crystallite order at the surface of the reference graphites, when compared to the graphitized AF samples. These differences in crystallite orientation seem to be related to the more developed three-dimensional microstructure (L_c values) of the R1−R3 graphites, rather than being affected by the bidimensional coalescence of the graphene layers (L_a values). In fact, the parameter I_D/I_t (recall Figure 1), which has been used systematically as an indication of the bidimensional crystallite order of carbon materials,[20,23−28] is greater for the reference graphites (12.9%, 18.4%, and 15.6% for R1, R2, and R3, respectively) than for the more graphitelike materials that are made from AF anthracite. It must be mentioned here that, apart from the extent of preferred orientation, there are other factors that contribute to the Raman D band intensity, such as the presence of amorphous carbon or doping.[20]

The helium density values in Table 1 were also sensitive to the microstructural evolution of the AF anthracite during the graphitization process. Moreover, they revealed crucial differences between the graphite materials that were prepared and the natural and synthetic graphites R1−R3. The helium densities of the graphitized AF samples had a tendency to increase as the treatment temperature increased, which is consistent with the evolution of the crystalline parameters. In other words, it gives an indication that more graphitelike materials are being produced from AF anthracite. However, the densities of the graphitized AF coal samples are still rather far from those of graphites R1−R3, which, in turn, are slightly greater than the theoretical value of 2.26 g/cm^3 determined for a perfect crystal of graphite. As mentioned in the Introduction, the presence of structural imperfections in the graphite materials, such as porosity, lattice defects, and dislocations, lead to lower densities. Because the most graphitelike materials from AF coal show a three-dimensional structural order that is comparable to the reference graphites, the development of significant porosity during the graphitization process, as observed by optical microscopy, may account for their lower densities. According to Blanche et al.,[15] lamellar microtextures with "imperfect" lamellae that still retained pore walls normal to the basal planes were observed after heat treatment of anthracites at temperatures up to 3073 K, even in the case of the strongly graphitizable anthracites.

Conclusions

The microstructural changes during the graphitization of an anthracite have been successfully monitored by means of X-ray diffraction and Raman spectroscopy. Interplanar distances and crystallite size measurements have been used to evaluate the degree of graphitization of the materials. Raman parameters such as the G bandwidths, D-band relative intensities (first-order region), the number of particles showing a G_1'/G_2' doublet, and the amount of its shift (second-order region) are sensitive features used to identify differences in orientation on the surface of highly ordered carbon materials.

The progress of the graphitization of the anthracite happens in two different stages. During the first stage, from 2273 to 2673 K, a relatively quick enhancement of the crystallite order and orientation of the graphite materials occurs. After a certain level of graphitization has been obtained, a further increase of the treatment temperature at >2673 K causes minor changes of the microstructural parameters. This behavior has been previously observed in the graphitization of other precursors that present a solid-phase type of carbonization (polyimides) and is explained in terms of a flattened-pore model.

The initial particle size of the anthracite affects the evolution of the graphitization process, relative to the temperature. Higher temperature is required for the graphitization of the anthracite with the smaller particle size to obtain materials with structural characteristics that are similar to those prepared from the anthracite with the larger particle size. The coal mineral matter is known to catalyze the graphitization process of the anthracite; therefore, this effect is most likely due to the decrease of the amount of particles with associations of organic matter and mineral matter during grinding.

The present anthracite shows a significant degree of graphitizability with crystalline parameters within the range of those observed for natural and other synthetic graphites. A main difference is the density of the graphite materials that are finally obtained, which are less dense than the reference graphites. This difference in density is explained in terms of the internal porosity that is developed during the graphitization of the anthracite.

Acknowledgment. Financial support from DGICYT (under Project No. MAT2001-1843) and FICYT (under Project No. PB-EXP01-01) is gratefully acknowledged. One of the authors (D.G.) thanks FICYT for a personal grant. Thanks are also due to Dr. M. A. Bañares of the Instituto de Catálisis, CSIC, Madrid (Spain) for providing access to the Raman spectrometer.

EF0300491